XRD and(29)Si MAS NMR study on carbonated cement paste under accelerated carbonation using different concentration of CO2

Citation for the original published paper (version of record):
Liu, W., Li, Y., Tang, L. et al (2019). XRD and(29)Si MAS NMR study on carbonated cement paste under accelerated carbonation using
different concentration of CO2. Materials Today Communications, 19(June): 464-470.
http://dx.doi.org/10.1016/j.mtcomm.2019.05.007

Materials Today Communications 19 (2019) 464–470

Contents lists available at ScienceDirect

Materials Today Communications

journal homepage: www.elsevier.com/locate/mtcomm

XRD and ^{29}Si MAS NMR study on carbonated cement paste under accelerated carbonation using different concentration of CO_2

Wei Liu[a], Yong-Qiang Li[a], Lu-Ping Tang[b], Zhi-Jun Dong[c,*]

[a] Guangdong Provincial Key Laboratory of Durability for Marine Civil Engineering, Shenzhen Durability Center for Civil Engineering, College of Civil and Transportation Engineering, Shenzhen, 518060, Guangdong, China
[b] Division of Building Technology, Chalmers University of Technology, 41296, Gothenburg, Sweden
[c] Institute of Technology for Marine Civil Engineering, Shenzhen Institute of Information Technology, Shenzhen, 518172, Guangdong, China

ARTICLE INFO

Keywords:
Cement
Carbonation
Different CO_2 concentration
XRD
^{29}Si MAS NMR

ABSTRACT

In this study, the chemical composition of cement pastes, exposed to accelerated carbonation using different concentration of CO_2 (3%, 10%, 20%, 50%,100%), have been determined and compared with those of natural carbonation (0.03%). Quantitative X-ray diffraction (QXRD) and ^{29}Si Magic Angle Spinning Nuclear Magnetic Resonance (MAS NMR) were used for characterisation and quantitative analysis of the carbonated phases. The obtained QXRD results revealed that the complete carbonation was hardly attained. Calcite, aragonite and vaterite were in co-existence after accelerated carbonation, while vaterite was dominant. The preferential polymorphic precipitation of the three crystal forms of calcium carbonate was affected by the carbonation degree of C-S-H and the duration of the carbonation process, but not by the concentration of CO_2. The NMR results indicated that C-S-H gel was strongly decalcified, and calcium modified silica gel was formed after carbonation. The C-S-H decalcification, under all the accelerated carbonation conditions, was clearly more pronounced than that under the natural carbonation conditions. When the concentration of CO_2 was in the range of 3%–20%, the ratio of decalcified to remaining C-S-H was similar, in a range of 5–6, while under the higher concentration of CO_2 this ratio was increased to > 8. Therefore, in consideration of both acceleration rate and measurement uncertainty, the higher concentration, up to 20%, of CO_2 in an accelerated carbonation should be applicable.

1. Introduction

Carbonation is one of the most well-discussed research topics in cement and concrete durability. Almost all the cement-based materials must undergo a certain extent of carbonation, during their whole service life, due to the presence of CO_2 in the atmosphere. The hydration phases, reacting with CO_2, mainly contain portlandite ($Ca(OH)_2$) and calcium-silicate-hydrate (C-S-H), which can be consumed simultaneously [1–4]. For hardened cement based materials, CO_2 can be dissolved into the pore solution to form carbonic acid, resulting in the consumption of $Ca(OH)_2$, which lowers the alkalinity and increases the possibility of corrosion of steel inside the concrete [5]. Meanwhile, when the $Ca(OH)_2$ is consumed, the calcium in the calcium-silicate-hydrate (C-S-H) will be released to try to maintain the alkaline environment needed for the C-S-H gel, resulting in the decalcification of C-S-H [6].

The carbonation reaction in a cement-based material, that occurs in the natural environment, is at a very slow rate due to the low concentration of CO_2 in the atmosphere (around 0.03% in volume) [7]. Accelerated carbonation experiments are commonly employed in the laboratory to evaluate the resistance of concrete to carbonation. National standards for accelerated carbonation varies between countries e.g. 1% in Belgium, 2% in Germany, 3% in the Nordic countries [8], 4% in the UK [9], and 20% in China [10]. Unfortunately, a universal standard for accelerated carbonation has not been established yet and some researchers are using even higher CO_2 concentrations in carbonation tests [11–13].

The strength of young concrete will be increased after carbonation [14–16] due to its effect of accelerating the hydration of C_3S and C_2S [17–19] and simultaneously reducing the porosity of concrete [20,21]. Also, the strength of aged concrete can be increased by the reaction products present in the carbonated system (i.e. Ca-modified silica gel and $CaCO_3$) because of their higher stiffness compared to the C-S-H phase [22,23]. The CO_2 concentration will affect the carbonation rate of concrete. In general, as Papadakis reported [24], the carbonation depth x_c can be predicted as the square root of the CO_2 concentration:

* Corresponding author.
E-mail address: dongzj@sziit.edu.cn (Z.-J. Dong).

https://doi.org/10.1016/j.mtcomm.2019.05.007
Received 12 March 2019; Received in revised form 15 May 2019; Accepted 15 May 2019
Available online 16 May 2019

$$x_c = A\sqrt{t} \quad (1)$$

$$A = \sqrt{\frac{2D_c[CO_2]^0}{[Ca(OH)_2]^0 + 3[CSH]^0 + 3[C_3S]^0 + 2[C_2S]^0}} \quad (2)$$

Where the D_c represents the effective diffusion coefficient of CO_2, $[CO_2]^0$ represents the concentration of CO_2, and the denominator in Eq. (2) is the total concentration of CaO in the form of carbonatable materials. However, in actual practice, the carbonation depths do not always obey the square root relationship with the CO_2 concentration. Cui et al. [25] have proved that the concrete carbonation depth increased with increasing CO_2 concentration, but the significance was markedly smaller when the CO_2 concentration was higher than 20%. They indicated that the mechanisms of CO_2 diffusion in concrete vary with different concentrations of CO_2 and they suggested that a dense carbonated microstructure would form, at the outermost layer of concrete, at a high concentration of CO_2. It was also reported by Loo et al. [26] that the carbonation rate apparently increased with increasing CO_2 concentration in the concrete with lower strength but this was not so significant in concrete with a strength higher than 40 MPa, because of the low rate of CO_2 diffusion.

This paper will focus on the effect of CO_2 concentration on the distribution of chemical phases after carbonation, i.e. calcium carbonate and decalcified C-S-H gel. The calcium carbonate can exist under several allotropic forms: calcite, aragonite and vaterite [27–31], with the possibility that amorphous calcium carbonate may also co-exist [32]. Researchers have found that mineralogical compositions of calcium carbonate, of concrete carbonated under natural conditions, and pure CO_2, are different [31,33,34]. Nevertheless, these studies only analysed the compositions in qualitative ways, and there is still a lack of quantitative analysis of the carbonated mineral phases. The decalcification of C-S-H gel, under natural and accelerated carbonation, has been studied using nuclear magnetic resonance (NMR) by several researcher [9,35–41], whereas NMR analysis about the decalcification of C-S-H gel, under different CO_2 concentrations, is rare and the resolution of NMR testing in the previous studies was not good enough for convincing deconvolution results [42]. The correlation between the effects of natural and accelerated carbonation, on cement-based materials, has so far remained unclear.

Therefore, it is necessary to study the carbonated phases under different CO_2 concentrations and find a CO_2 concentration, which not only has the best efficiency for accelerating carbonation, but also does not dramatically change the distribution of the carbonated phases. The morphology of calcium carbonate, and decalcification of C-S-H gel, should be quantitatively analysed to give direct evidence of the effect of different CO_2 concentrations. In the present work, cement paste was exposed to natural carbonation (0.03% CO_2) and accelerated carbonation at different concentrations of CO_2 (3%, 10%, 20%, 50% and 100%), the concentration being precisely controlled via a newly developed controller. X-ray diffraction (XRD) and ^{29}Si magic angle spinning nuclear magnetic resonance (MAS-NMR) measurements were employed in this study for quantitative analysis of the carbonated phases under different CO_2 concentrations.

2. Materials and preparation

In this study a type of Chinese reference Portland cement was used to ensure the traceability of chemical compositions. The cement was fabricated by China United Cement Corporation and complied with the requirements according to Chinese standard GB8076-2008. Its chemical composition is listed in Table 1. Fig. 1 shows the particle size distribution of the cement powder as measured by HELOS (H3585) laser particle size analyser. The D50, D90 and D(4,3) are 13.39 μm, 4.45 μm and 19.01 μm, respectively, according to the analysis.

Cement paste samples were prepared by mixing de-ionised water with the reference cement with the water/cement ratio being 0.56. The samples were cast in plastic tubes (∅10 mm × 100 mm) and put in a rotating apparatus, at a speed of 10 rpm/min for 24 h, to remove entrapped air bubbles. The samples were then cured in the room at 22°C for three months in a sealed condition. Afterwards the cement samples were demoulded by using an endotherm knife and cut into small cylinders of size ∅10 mm × 10 mm using a diamond sawing machine. Finally, the cylinders were put into a carbonation environment.

Table 1
Chemical compositions of reference cement (wt%).

SiO_2	Al_2O_3	Fe_2O_3	CaO	MgO	SO_3	Na_2O	Free CaO	Loss	Cl^-
21.98	4.51	3.55	64.45	2.40	2.45	0.502	0.9	1.22	0.01

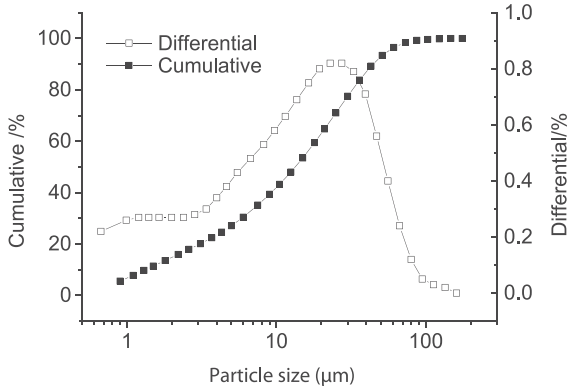

Fig. 1. Particle size distribution of cement powder.

A new chamber was designed for accelerated carbonation as shown in Fig. 2. In the carbonation chamber, a designated concentration of CO_2 was achieved by mixing pure CO_2 gas with fresh air. An electronic sensor, sensitive to CO_2 with a precision of 0.01%, was put inside the chamber to measure the concentration of carbon dioxide. A magnetic valve, operated by a computerised controller, was used to control the in-flow of CO_2. Once the desired concentration was reached, the valve was closed to maintain the experimental conditions. According to the data, monitored during the tests, the variation of CO_2 concentration was in a range of 0.5%.

The relative humidity inside the chamber was controlled as 74 ± 2% by a saturated $NaNO_3$ solution. The environmental temperature was set as 20 ± 2°C through an air conditioner. The concentration of CO_2 was set at 3%, 10%, 20%, 50% and 100%, respectively. Meanwhile, the parallel batch of cement samples were carbonated in the fresh air condition (around 0.03% of CO_2) for 60 days, where relatively humidity was ranging from 40% to 75% and average temperature was 25°C.

During carbonation, some of the samples were taken out, at certain intervals, for checking on the carbonation depth by cutting and spraying with a phenolphthalein solution. The carbonation was deemed

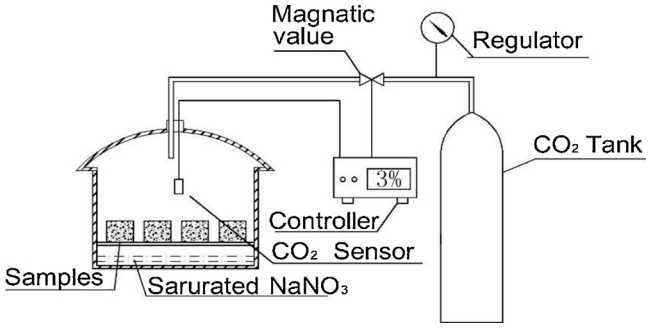

Fig. 2. Sketch of carbonation device.

to have finished when the whole cutting faces were colourless (pH ≤ 9) after spraying with the phenolphthalein solution. It was observed that the cutting faces became colourless when sprayed with phenolphthalein solution after just 3 days carbonation. In order to ensure enough carbonation, the carbonation time for 100% CO_2 sample was lengthened to 14 days, whilst for the other samples, the carbonation process was sustained for 60 days. The carbonation depth in the samples exposed to the natural environment was only about 3 mm.

When the carbonation process was finished, the samples subjected to the accelerated carbonation were crushed to powder with an agate mortar and sieved through a sieve of 0.25 mm. For the sample carbonated in the natural environment, the carbonation depth was about 3 mm. The powder for analysis was gently scraped from the first 1 mm of carbonated area using a blade. Therefore, the containment of uncarbonated cement should have been avoided.

3. Analysis methods

3.1. ^{29}Si magic angle spinning nuclear magnetic resonance

Dipolar Decoupling Magic angle spinning (DDMAS) nuclear magnetic resonance (NMR) with ^{29}Si was used for detecting the structural changes of C-S-H gel after carbonation. Spectra were collected by JEOL ECZ600MHz (14.1 T) spectrometer, with a spinning speed of 15 kHz in a 3.2 mm ZrO_2 rotors, $\Upsilon B/2\pi = 40$ kHz. The relaxation delay was chosen as 10 s because no significant difference in spectra was found when this parameter was set between 10 s, 20 s, 30 s, 60 s and 100 s. The number of scans was set as 8500. Trimethylsilyl (TSPA) was used as an external reference. The spectrum was analysed to obtain information, regarding the peaks, related to the silicate configuration.

3.2. X-ray diffraction (XRD) analysis

Bruker D8 Advance powder diffractometer with Cu K_α radiation (40kv and 40 mA, scan interval 5-70° 2θ, with a step of 0.0194° and 1 s per step) was employed for identifying mineral compositions of cement pastes carbonated under different concentrations of CO_2. Phase identification was performed using EVA software. TOPAS software was used for Rietveld refinement quantitative analysis of all the mineral phases except the C-S-H which was not counted due to the lack of a suitable model structure [43]. The fitting accuracy of quantitative analysis was kept at $R_{wp} < 10\%$.

4. Result and discussion

4.1. XRD results

Fig. 3 shows the diffractograms of the samples carbonated under different CO_2 concentrations. Here, only the main phases related to carbonation process were marked. The reference sample refers to the uncarbonated sample. Portlandite was found as the main phase in the reference sample. When cement samples were carbonated, calcium carbonate was formed with three kinds of polymorph (vaterite, calcite, aragonite), though the signal of aragonite is nearly untraceable in the diffractograms. It can be seen that, in the natural air condition (0.03%), both vaterite and calcite show a high intensity. However, in the accelerated conditions, vaterite becomes the major precipitated phase whilst calcite shows a relatively low intensity.

The results from the quantitative analysis by using Rietveld refinement are shown in Table 2. The results show that the total amount of calcium carbonate, in the sample carbonated under 0.03% CO_2, represented 88.8% of the total amount of detectable phases, which was increased to a range of 94% and 95.6% under the accelerated carbonation. Meanwhile, the portlandite was almost undetectable after the accelerated carbonation. The amount of calcite, in the sample after carbonation under 0.03% CO_2, was 38.7% of the total amount of

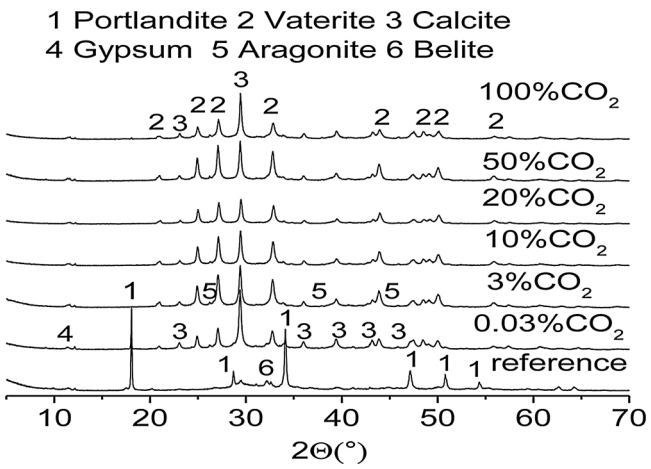

Fig. 3. Diffractograms of cement pastes after carbonation under different concentration of CO_2.

Table 2
Rietveld refinement results of the composition of cement samples after carbonation under different concentration of CO_2 (wt%, not accounting for C-S-H gel, p = portlandite, e = ettringite, g = gypsum, c = calcite, a = aragonite, v = vaterite).

Sample	p	e	g	c	a	v	c + a + v	others
Reference	56.8	0.4	3.9	0	0	0	0	38.9
0.03% CO_2	0.9	0.8	1.1	38.7	1.3	48.8	88.8	8.4
3% CO_2	0	0.2	1	21.8	0.1	73.7	95.6	3.2
10% CO_2	0	0.3	1	22	0.7	74	96.7	2
20% CO_2	0	0.2	1	20.9	0.9	73.2	95	3.8
50% CO_2	0	0.2	1.1	19.6	0.3	75.7	95.6	3.1
100% CO_2	0.1	0.1	1.4	31.7	1.4	60.9	94	4.4

detectable phases, whilst this amount was reduced to around 20% of the total amount of detectable phases in the accelerated carbonation, except for the 100% CO_2 condition. Vaterite was the dominating precipitate in carbonated phases with about 50%, and more than 73%, of the total amount of detectable phases in the samples after the natural carbonation and the accelerated carbonation (except for 100% CO_2 condition), respectively.

4.2. ^{29}Si MAS NMR results

Deconvolution results of ^{29}Si MAS NMR spectra after the carbonation of the cement samples under different concentrations of CO_2 are shown in Fig. 4. The ^{29}Si MAS NMR spectrum gives the proportion of Q_n (n = 0, 1, 2, 3, 4), where Q_n represents a Si atom bonded through oxygen to other Si atoms [44]. Four peaks were found in the reference sample. The peak with the maximum intensity, locked at -71 ppm, was marked as Q_0, originating from C_3S and C_2S [9,42,45]. Q_1 (around -80 ppm) and Q_2 (around -85.5 ppm) represent the chemical environment of silicon atoms in the C-S-H, which belong to chain-end groups or dimers and chain middle groups, respectively [45]. Also, the small amount of Q_3(Ca) (1.6%) at -93 ppm which occurred, was attributed to the cross-linked silicate tetrahedrons, which increase dramatically after carbonation. Two broader and overlapping peaks were seen after carbonation. The peak assigned at −101 ppm was Q_3(OH) (hydroxylated surface sites $(SiO)_3$-Si-OH), whilst the peak at around −110 ppm was Q_4 (fully condensed network of silicate tetrahedrons) [7,37].

The relative intensities (Q_n%) from the deconvolution results are given in Table 3. It can be seen that the compositions of Q_0, Q_1 and Q_2 were obviously reduced after carbonation. However, a small amount of Q_0 still remained after carbonation for 60 days, which could be due to the extremely slow carbonation rate of the un-hydrated C_2S and C_3S

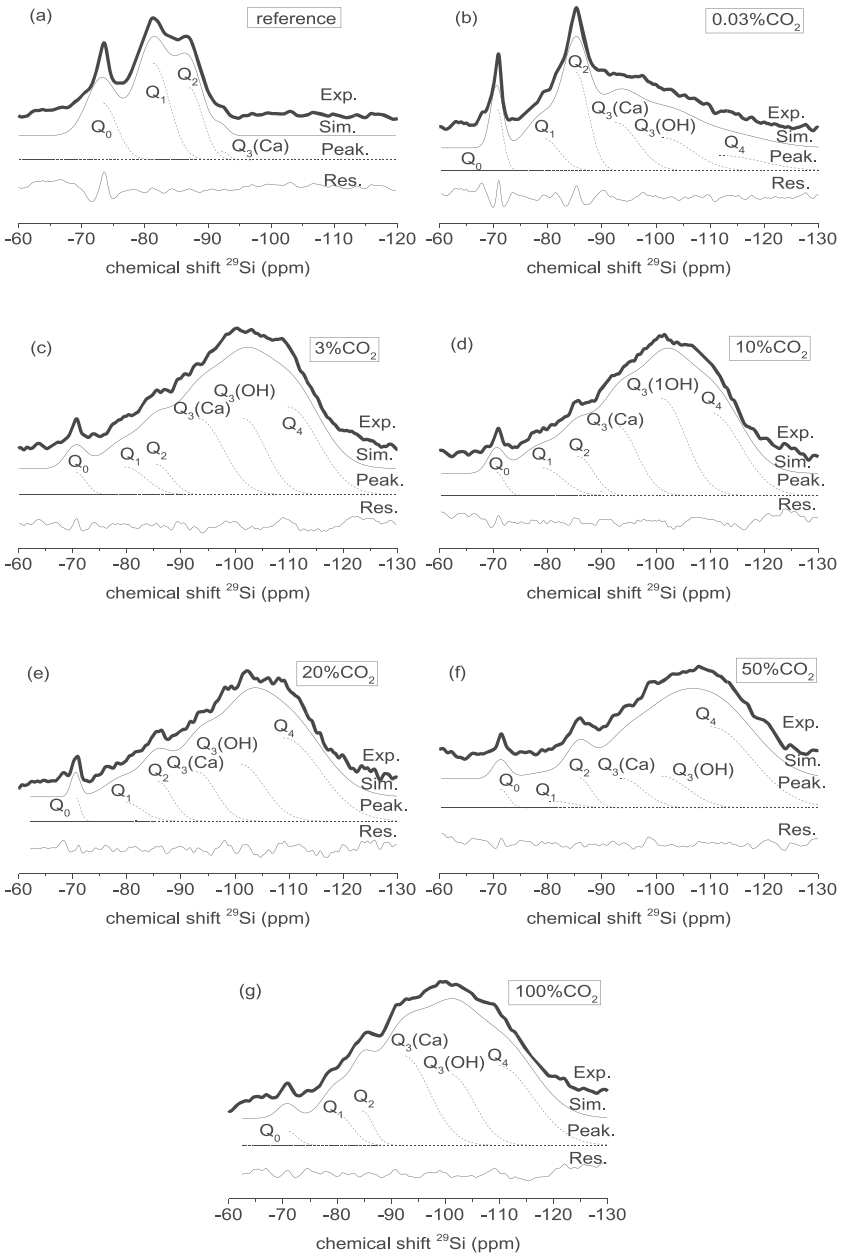

Fig. 4. ^{29}Si MAS NMR spectra of samples after carbonation under different concentration of CO_2 (Exp. = experimental result, Sim. = simulated spectra, Peak. = separating simulated peaks, Res. = difference between experimental and simulated result).

Table 3
Composition of samples given by ^{29}Si MAS NMR after carbonation under different concentration of CO_2 (%).

Sample	Unhydrated	C-S-H		Ca-modified silica gel		
	Q_0(%)	Q_1(%)	Q_2(%)	Q_3(Ca)(%)	Q_3(OH)(%)	Q_4(%)
Reference	24.9	45.4	28.1	1.6		
0.03% CO_2	8.2	10.9	25.9	22.0	20.1	12.9
3% CO_2	3.0	7.5	5.9	25.1	23.1	35.4
10% CO_2	2.6	7.6	8.1	18.6	30.6	32.5
20% CO_2	1.7	5.3	8.9	14.4	21.7	48
50% CO_2	2.6	6.6	2.9	11.8	15	61.1
100% CO_2	1.8	5.9	4.6	30.2	21.2	36.3

[2,46]. The reduction of Q_1 and Q_2 as well as the appearance of Q_3(Ca), Q_3(OH) and Q_4 indicate the decalcification of C-S-H gel. By using the following equation, the level of decalcification could be evaluated with a ratio L_d by comparing the relative intensities related to C-S-H (Q_1, Q_2) before (superscript 'b') and after (superscript 'a') carbonation [9]:

$$L_d = \left(1 - \frac{Q_1^a + Q_2^a}{Q_1^b + Q_2^b}\right) \times 100\% \quad (3)$$

The results shown in Table 4 clearly confirm the strong decalcification of C-S-H. For the reference sample, C-S-H occupies more than 70% of the total amount of phases. L_d varies from 50% to 87% after carbonation under different concentrations of CO_2, showing that only a small amount of C-S-H remained after carbonation (9.5% to 36.8%). It should be noted that little C-S-H remained after carbonation where the corresponding solution pH was more than 10 [47,48], though the paste showed as colourless with the phenolphthalein solution, which is consistent with the findings in previous studies [9,42]. Furthermore, as Table 4 shows, the L_d for samples carbonated at 50% and 100% CO_2 (87.1% and 85.7% respectively) were larger than that at 3%, 10% and 20% CO_2 (around 80%), which may be explained by the

Table 4
Calculation of remained C-S-H and decalcified C-S-H after carbonation.

Sample	Q_1+Q_2(%)	$Q_3(Ca)+Q_3(OH)+Q_4$(%)	L_d(%)	B/A[a]
Reference	73.5	1.6	0	0.02
0.03% CO_2	36.8	55	49.93	1.49
3% CO_2	13.4	83.6	81.77	6.24
10% CO_2	15.7	81.7	78.64	5.20
20% CO_2	14.2	84.1	80.68	5.92
50% CO_2	9.5	87.9	87.07	9.25
100% CO_2	10.5	87.7	85.71	8.35

[a] $A = Q_1+Q_2$, $B = Q_3(Ca)+Q_3(OH)+Q_4$.

increased availability of CO_2 under a high concentration of CO_2.

5. Discussion

The CO_2 concentration for accelerated carbonation tests varies between different countries. Usually, 3% is chosen as this is considered as the condition relatively close to the natural one [9,49]. In this paper, the difference of chemical compositions between the natural condition (0.03% CO_2) and accelerated conditions (3%, 10%, 20%, 50% and 100% CO_2) has been studied. Calcite should be thermodynamically stable at room temperature and pressure [50]. However, in a Portland cement system, after carbonation, vaterite was the dominant phase whose content is more than calcite even under the natural air carbonation. Therefore, the formation of calcium carbonate in cement-based materials was different from that expected according to classic chemical reactions. The presence of vaterite and aragonite was an intrinsic feature of carbonation.

It has been indicated by Auroy et al. [9] that calcite and aragonite will be precipitated after the carbonation of both C-S-H and portlandite, whereas vaterite was only precipitated from the carbonation of C-S-H. As shown in Table 4, the remaining C-S-H (i.e. Q_1+Q_2) in 0.03% CO_2 was 36.8%, a value that decreased to a range of 9.5% and 15.7% under accelerated carbonation. Thus, in this study, the lower content of vaterite, in the natural condition (0.03% CO_2), should be attributed to the low de-calcification degree of C-S-H in cement paste. Nevertheless, for samples carbonated at 100% CO_2, the content of calcite (31.7%) and vaterite (60.9%) were different from those in 3%–50% CO_2 conditions, though the content of remaining C-S-H (10.5%) was similar within samples of other accelerated conditions. This may be explained by the shortage of carbonation time (only 14 days) for the sample in the 100% CO_2 condition. If the carbonation time was prolonged to 60 days, the content of calcite and vaterite would be expected to have the same value as that in 3%–50% CO_2 conditions. It is worth to emphasising that the XRD results revealed quite similar quantities of calcite, aragonite and vaterite in the samples carbonated under the accelerated conditions below 50% CO_2, which is evidence that the preferential polymorphic precipitation of calcium carbonate was affected by the carbonation degree of C-S-H and the duration of the carbonation process, but not by the concentration of CO_2.

Rietveld refinement results in Table 2 show that portlandite remained in the cement matrix under the natural condition (0.03% CO_2) but vanished in the accelerated conditions. In fact, the powder in this study was ground from an area where phenolphthalein spraying showed colourless, with the expectation that the entire portlandite had been consumed after carbonation. The remaining portlandite, under the natural condition, can be attributed to the formation of a slightly diffusive calcium carbonate layer around the grains of portlandite that hindered their dissolution, indicating that the carbonation process never reached the ultimate state in the natural condition (0.03% CO_2). This is consistent with previous studies [9,33,40,51]. However, the remaining portlandite content was so small as to be negligible. For the accelerated conditions, the carbonation time was prolonged for more than the time when phenolphthalein spraying tests showed colourless on the cutting surface so that carbonation was deemed to be enough. The portlandite content, under accelerated conditions, almost vanished, which could also illustrate the sufficiency of the carbonation.

The C-S-H gel, defined as Q_1 and Q_2 in the NMR analysis, which is responsible for the main strength of cement paste, was shown to remain in all samples, after accelerated carbonation conditions, though most of it was decalcified to calcium modified silicate gel. It is reported that [35], during the carbonation process, C-S-H gel was decalcified by the removal of inter-layer Ca ions (i.e., Ca at the interlayer sites balancing silicate anions). The excess negative charge, caused by removal of interlayer Ca ions, is then balanced through protonation and subsequent formation of Si-OH which then condense according to Eq. (4) [52].

$$\equiv Si- OH+ OH- Si\equiv \rightarrow \equiv Si- O- Si\equiv + H_2O \quad (4)$$

This condensation should be responsible for the amorphous silica phases Q_3 and Q_4 seen in the NMR results, meanwhile increasing the average length of silica chain. For C-S-H with a Ca/Si ratio higher than 0.67 [53,54], the decomposition of the C-S-H gel involves two steps, corresponding to the follow ideal reaction schemes [35]:

$$(CaO)_{x+0.67}SiO_2(H_2O)_y + xCO_2 \rightarrow (CaO)_{0.67}SiO_2(H_2O)_{y-z} + xCaCO_3 \quad (5)$$

$$(CaO)_{0.67}SiO_2(H_2O)_{y-z} + xCO_2 \rightarrow 0.67CaCO_3 + SiO_2(H_2O)_{y-z-n} \quad (6)$$

where $0 \leqq x \leqq 1.1$, $0.4 \leqq y \leqq 2.5$. In this study, the initial Ca/Si ratio in the cement paste was about 1.7, which was de-calcified first to a Ca/Si ratio of 0.67, then further decomposed to silica gel according to Eq. (6). This means that uncarbonated, decalcified and decomposed parts of C-S-H were mixed in the cement matrix. The pH of corresponding aqueous solution of C-S-H gel with 0.67 Ca/Si was about 10 [47,48], which does not match the colourless condition of phenolphthalein solution spraying (pH ≤ 8.9), that is, the reaction in Eq. (5) has been finished and the C-S-H has been decomposed to the calcium-modified silica gel which made the pH in the pore solution lower than 8.9.

The remaining content of C-S-H (Q_1+Q_2) and the decalcification degree of C-S-H (L_d) is presented in Table 4. As the results show, a lot of the C-S-H was un-decalcified after the natural carbonation, indicating the slow rate of decalcification at the low carbonation concentrations. Besides, the C-S-H levels remaining, under the carbonations of 3%, 10% and 20% CO_2, are quite similar and higher than those in 50% and 100% CO_2, suggesting a similar carbonation environment in 3%, 10% and 20% CO_2. Assuming the Tobermorite–like model for the C-S-H structure [55], the C-S-H should be decalcified to $Q_3(Ca)$ ($(SiO\text{-})_3Si^*$-1/2Ca, -93 ppm) and $Q_3(OH)$ ($(SiO\text{-})_3Si^*$-OH, -101 ppm) groups first during carbonation and then be decalcified to the full condensed group Q_4 ($(SiO\text{-})_4Si^*$, −110 ppm) by further carbonation.

The total content of decalcified C-S-H ($Q_3(Ca)+Q_3(OH)+Q_4$) and the ratio of decalcified to remained C-S-H (B/A) are summarised in Table 4. It can be seen that, under the accelerated conditions from 3% to 20% CO_2, the ratio of decalcified to remained C-S-H was similar, that is, B/A = 5-6, while under the higher CO_2, this ratio was increased to more than 8. Therefore, it is reasonable to assume the similar degree of decalcification for C-S-H under the accelerated conditions at the concentration of CO_2 between 3% to 20%.

However, the actual concentrations of CO_2 in the test chamber are not always as stable as expected. In this study, the variation of actual concentration in the chamber was recorded as ± 0.5%, which contributes to 16.7%, 5% and 2.5% target errors for concentration of 3%, 10% and 20% CO_2, respectively. If the carbonation test was performed at a low concentration, the measurement precision will be impaired dramatically due to the uncertainty of CO_2 concentration, as mentioned previously by Harrison et al. [56]. It is clear from the view point of measurement uncertainty, that the higher CO_2 concentration will contribute to a better precision.

Therefore, considering the similar degree of decalcification for C-S-H the accelerated carbonation test under the concentration of 20% CO_2

should provide the most precise measurements.

It should be noted that NMR results in this study are more suitable for cement with low content of aluminium. If cement is blended with supplementary cementitious materials, such as fly ash or slag, the Al incorporated in C-S-H should be considered and ^{27}Al MAS NMR can be applied for further analysis [57].

6. Conclusions

Accelerated carbonation experiments are commonly used in laboratory by increasing the concentration of CO_2 and standards for that are varies from different countries. In this study, microstructural changes of cement paste, after carbonation using different concentration of CO_2, were investigated by ^{29}Si DDMAS-NMR and XRD analysis. The samples were tested after complete carbonation.

Though phenolphthalein indicator showed colourless after only a few days under the accelerated carbonation, portlandite and C-S-H gel remained in the carbonated samples. Full carbonation could not be reached, even after 60 days, under the accelerated carbonation with 50% CO_2. However, considering the small amount of portlandite and C-S-H left, the carbonation degree in this study can be considered as being enough.

The results from XRD analysis have revealed preferential polymorphic precipitation of three crystal forms of calcium carbonate, namely calcite, aragonite and vaterite. Among them, vaterite is the dominant phase. This preferential polymorphic precipitation of calcium carbonate was affected by the carbonation degree of C-S-H and the duration of carbonation process, but not by the concentration of CO_2.

The NMR results showed that C-S-H gel was strongly decalcified, and calcium modified silica gel was detected after carbonation. The decalcification of C-S-H was more obvious in the accelerated conditions. After carbonation, C-S-H gel, decalcified C-S-H gel and decomposed C-S-H gel are in co-existence. The ratio of remaining to decalcified C-S-H, under the accelerated carbonation conditions, is always higher than that under the natural conditions, but they are similar when the concentration of CO_2 was in the range of 3% and 20%.

Considering the similar degree of decalcification for C-S-H the accelerated carbonation test under the concentration of 20% CO_2 should provide the most precise measurements.

Data availability

The raw/processed data are available at https://doi.org/10.17632/vpphrvnf45.2.

Acknowledgements

The work described in this paper was fully supported by grants from Natural Science Foundation of China (51678368 and 51478271) and Key Project of DEGP (No. 2014KZDXM051).

References

[1] W.J. Long, Y.C. Gu, F. Xing, et al., Microstructure development and mechanism of hardened cement paste incorporating graphene oxide during carbonation, Cem. Concr. Compos. 94 (2018) 72–84.
[2] Q.Z. Shen, G.H. Pan, B.F. Bao, A method for calculating the carbonation degree of calcium–silicate–hydrate, Adv. Cem. Res. 30 (2018) 427–436.
[3] X.F. Wang, C. Fang, D.W. Li, et al., A self-healing cementitious composite with mineral admixtures and built-in carbonate, Cem. Concr. Compos. 92 (2018) 216–229.
[4] W.J. Long, X.W. Tan, B.X. Xiao, et al., Effective use of ground waste expanded perlite as green supplementary cementitious material in eco-friendly alkali activated slag composites, J. Clean. Prod. 213 (2019) 406–414.
[5] C. Alonso, C. Andrade, J.A. González, Relation between resistivity and corrosion rate of reinforcements in carbonated mortar made with several cement types, Cem. Concr. Res. 18 (1988) 687–698.
[6] H.Y. Ma, Multi-scale Modeling of the Microstructure and Transport Properties of Contemporary Concrete, The Hong Kong University of Science and Technology, Hong Kong, 2013.
[7] W. Ashraf, Carbonation of cement-based materials: challenges and opportunities, Constr. Build. Mater. 120 (2016) 558–570.
[8] NORDTEST, Concrete, Repairing Materials and Protective Coating Carbonation Resistance, NT BUILD 357, Finland, 1989.
[9] M. Auroy, S. Poyet, P. Le Bescop, et al., Comparison between natural and accelerated carbonation (3% CO_2): impact on mineralogy, microstructure, water retention and cracking, Cem. Concr. Res. 109 (2018) 64–80.
[10] GB/T50082-2009, Standard for Test Methods of Long-term Performance and Durability of Ordinary Concrete, Ministry of Housing and Urban-Rural Development of the People's Republic of China, Beijing, 2009.
[11] C.F. Chang, J.W. Chen, The experimental investigation of concrete carbonation depth, Cem. Concr. Res. 36 (2006) 1760–1767.
[12] P.h. Turcry, L. Oksri-Nelfia, A. Younsi, et al., Analysis of an accelerated carbonation test with severe preconditioning, Cem. Concr. Res. 57 (2014) 70–78.
[13] T. Gonen, S. Yazicioglu, The influence of compaction pores on sorptivity and carbonation of concrete, Constr. Build. Mater. 21 (2007) 1040–1045.
[14] M.A. Sanjuán, C. Andrade, M. Cheyrezy, Concrete carbonation test in natural and accelerated conditions, Adv. Cem. Res. 15 (2003) 171–180.
[15] V. Rostami, Y.X. Shao, A.J. Boyd, Carbonation curing versus steam curing for precast concrete production, J. Mater. Civil. Eng. 24 (2012) 1221–1229.
[16] J.M. Chi, R. Huang, C.C. Yang, Effects of carbonation on mechanical properties and durability of concrete using accelerated testing method, J. Mar. Sci. Technol. Jpn. 10 (2002) 14–20.
[17] R.L. Berger, J.F. Young, K. Leung, Acceleration of hydration of calcium silicates by carbon dioxide treatment, Nat. Phys. Sci. 240 (1972) 16–18.
[18] J.F. Young, R.L. Berger, J. Breese, Accelerated curing of compacted calcium silicate mortars on exposure to CO_2, J. Am. Ceram. Soc. 57 (1974) 394–397.
[19] J.M. Bukowski, R.L. Berger, Reactivity and strength development of CO_2 activated non-hydraulic calcium silicates, Cem. Concr. Res. 9 (1979) 57–68.
[20] S.E. Pihlajavaara, Some results of the effect of carbonation on the porosity and pore size distribution of cement paste, Mater. Struct. 1 (1968) 521–527.
[21] V.T. Ngala, C.L. Page, Effects of carbonation on pore structure and diffusional properties of hydrated cement pastes, Cem. Concr. Res. 27 (1997) 995–1007.
[22] W. Ashraf, J. Olek, Carbonation activated binders from pure calcium silicates: reaction kinetics and performance controlling factors, Cem. Concr. Compos. 93 (2018) 85–98.
[23] W. Ashraf, J. Olek, Carbonation behavior of hydraulic and non-hydraulic calcium silicates: potential of utilizing low-lime calcium silicates in cement-based materials, J. Mater. Sci. 51 (2016) 6173–6191.
[24] V.G. Papadakis, C.G. Vayenas, M.N. Fardis, Fundamental modeling and experimental investigation of concrete carbonation, ACI Mater. J 88 (1991) 363–373.
[25] H.Z. Cui, W.C. Tang, W. Liu, et al., Experimental study on effects of CO_2 concentrations on concrete carbonation and diffusion mechanisms, Constr. Build. Mater. 93 (2015) 522–527.
[26] Y.H. Loo, M.S. Chin, C.T. Tam, et al., A carbonation prediction model for accelerated carbonation testing of concrete, Mag. Concr. Res. 46 (1994) 191–200.
[27] W.F. Cole, B. Kroone, Carbonate minerals in hydrated Portland cement, Nature 184 (1959) 57.
[28] H. El-Hassan, Y.X. Shao, Early carbonation curing of concrete masonry units with Portland limestone cement, Cem. Concr. Compos. 62 (2015) 168–177.
[29] V. Lilkov, I. Rostovsky, O. Petrov, et al., Long term study of hardened cement pastes containing silica fume and fly ash, Constr. Build. Mater. 60 (2014) 48–56.
[30] J. Chang, Y.F. Fang, Quantitative analysis of accelerated carbonation products of the synthetic calcium silicate hydrate(C–S–H) by QXRD and TG/MS, J. Therm. Anal. Calorim. 119 (2014) 57–62.
[31] S. Goni, M.T. Gaztañaga, A. Guerrero, Role of cement type on carbonation attack, J. Mater. Res. 17 (2002) 1834–1842.
[32] W. Ashraf, J. Olek, Elucidating the accelerated carbonation products of calcium silicates using multi-technique approach, J. CO_2 Util. 23 (2018) 61–74.
[33] D.J. Anstice, C.L. Page, M.M. Page, The pore solution phase of carbonated cement pastes, Cem. Concr. Res. 35 (2005) 377–383.
[34] Z. Sauman, Carbonization of porous concrete and its main binding components, Cem. Concr. Res. 1 (1971) 645–662.
[35] T.F. Sevelsted, J. Skibsted, Carbonation of C–S–H and C–A–S–H samples studied by ^{13}C, ^{27}Al and ^{29}Si MAS NMR spectroscopy, Cem. Concr. Res. 71 (2015) 56–65.
[36] J.J. Chen, J.J. Thomas, H.M. Jennings, Decalcification shrinkage of cement paste, Cem. Concr. Res. 36 (2006) 801–809.
[37] S. Thomas, K. Meise-Gresch, W. Müller-Warmuth, et al., MAS NMR studies of partially carbonated portland cement and tricalcium silicate pastes, J. Am. Ceram. Soc. 76 (2005) 1998–2004.
[38] N. Li, N. Farzadnia, C.J. Shi, Microstructural changes in alkali-activated slag mortars induced by accelerated carbonation, Cem. Concr. Res. 100 (2017) 214–226.
[39] J.H. Seo, S.M. Park, H.K. Lee, Evolution of the binder gel in carbonation-cured Portland cement in an acidic medium, Cem. Concr. Res. 109 (2018) 81–89.
[40] G.W. Groves, A. Brough, I.G. Richardson, et al., Progressive changes in the structure of hardened C_3S cement pastes due to carbonation, J. Am. Ceram. Soc. 74 (1991) 2891–2896.
[41] F. Matsushita, Y. Aono, S. Shibata, Calcium silicate structure and carbonation shrinkage of a tobermorite-based material, Cem. Concr. Res. 34 (2004) 1251–1257.
[42] M. Castellote, L. Fernandez, C. Andrade, et al., Chemical changes and phase analysis of OPC pastes carbonated at different CO2 concentrations, Mater. Struct. 42 (2008) 515–525.
[43] I. Richardson, Model structures for C-(A)-S-H(I), Acta Crystallogr. 70 (2015) 903–923.
[44] A.J. Vega, G.W. Scherer, Study of structural evolution of silica gel using ^{1}H and ^{29}Si

NMR, J. Non-Cryst. Solids 111 (1989) 153–166.
[45] Y. Ikeda, Y. Yasuike, M. Kumagai, et al., ^{29}Si MAS NMR study on structural change of silicate anions with carbonation of synthetic 11Å tobermorite, J. Ceram. Soc. Jan. 100 (1992) 1098–1102.
[46] J. Hjorth, J. Skibsted, H.J. Jakobsen, ^{29}Si MAS NMR studies of portland cement components and effects of microsilica on the hydration react, Cem. Concr. Res. 18 (1988) 789–798.
[47] B. Lothenbach, A. Nonat, Calcium silicate hydrates: solid and liquid phase composition, Cem. Concr. Res. 78 (2015) 57–70.
[48] C.S. Walker, D. Savage, M. Tyrer, et al., Non-ideal solid solution aqueous solution modeling of synthetic calcium silicate hydrate, Cem. Concr. Res. 37 (2007) 502–511.
[49] V. Shah, K. Scrivener, B. Bhattacharjee, et al., Changes in microstructure characteristics of cement paste on carbonation, Cem. Concr. Res. 109 (2018) 184–197.
[50] J. Kawano, N. Shimobayashi, A. Miyake, et al., Precipitation diagram of calcium carbonate polymorphs: its construction and significance, J. Phys. Condens. Matter 21 (2009).
[51] G.W. Groves, D.I. Rodway, I.G. Richardson, The carbonation of hardened cement pastes, Adv. Cem. Res. 3 (1990) 117–125.
[52] M. Monasterio, J.J. Gaitero, E. Erkizia, et al., Effect of addition of silica- and amine functionalized silica-nanoparticles on the microstructure of calcium silicate hydrate (C-S-H) gel, J. Colloid Interface Sci. 450 (2015) 109–118.
[53] L. Black, C. Breen, J. Yarwood, et al., Structural features of C-S-H(I) and its carbonation in air—a Raman spectroscopic study. Part II: carbonated phases, J. Am. Ceram. Soc. 90 (2007) 908–917.
[54] L. Black, K. Garbev, I. Gee, Surface carbonation of synthetic C-S-H samples: a comparison between fresh and aged C-S-H using X-ray photoelectron spectroscopy, Cem. Concr. Res. 38 (2008) 745–750.
[55] I.G. Richardson, G.W. Groves, Models for the composition and structure of calcium silicate hydrate (C–S–H) gel in hardened tricalcium silicate pastes, Cem. Concr. Res. 22 (1992) 1001–1010.
[56] T.A. Harrison, M.R. Jones, M.D. Newlands, et al., Experience of using the prTS 12390-12 accelerated carbonation test to assess the relative performance of concrete, Mag. Concrete. Res. 64 (2012) 737–747.
[57] M.D. Andersen, H.J. Jakobsen, J. Skibsted, Characterization of white Portland cement hydration and the C-S-H structure in the presence of sodium aluminate by ^{27}Al and ^{29}Si MAS NMR spectroscopy, Cem. Concr. Res. 34 (2004) 857–868.